Heliyon 10 (2024) e39080

Contents lists available at ScienceDirect

Heliyon

journal homepage: www.cell.com/heliyon

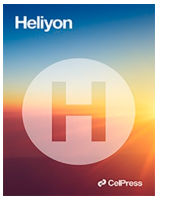

Research article

Removal of zinc from wastewaters using Turkish bentonite and artificial neural network [ANN] modeling

Ezel Uraz, Tugba Hayri-Senel, Nalan Erdol-Aydin *, Gulhayat Nasun-Saygili

Istanbul Technical University, Chemical and Metallurgical Faculty, Chemical Engineering Department, 34469, Maslak, Istanbul, Turkey

ARTICLE INFO

Keywords:
Adsorption
Bentonite
Zinc
Isotherm models
Artificial neural networks
Modeling
Optimization

ABSTRACT

In this study, Ordu-Unye bentonite was used as an adsorbent in the removal of zinc from aqueous solutions. The aim of the experimental part of the study was to ascertain how zinc removal was affected by variables such as pH, adsorbent amount, contact time, and initial zinc concentration. In the second part of the experiments, bentonite was modified with two different acids and the adsorption performance of modified bentonite was also investigated. Characterization of raw and modified bentonites was also carried out using FTIR and XRD. It was observed that acid modification of bentonite negatively affected the zinc removal process from aqueous solutions. In this study, higher zinc removal (95 %) was obtained with raw bentonite compared to acid modified bentonites (58.4 % in HNO_3 activated, 43.8 % for H_2SO_4 activated). Equilibrium isotherms were obtained and modelled to explain the adsorption mechanism. Adsorption isotherm studies showed that zinc adsorption fits well with Langmuir (R^2: 0.99) and Temkin (R^2: 0.97) models. Besides from these experimental investigations, various artificial neural network (ANN) training techniques were used to optimize the zinc adsorption process. By trial and error, the optimal performance was obtained by changing the number of hidden neurons in each layer of the neural network architecture. These models under study were analyzed to determine their R^2 and mean square error (MSE) values, and the optimal outcomes were identified. Among the various training models of ANN, it was determined that the Bayesian Regularization method exhibited the optimum network architecture with the highest R^2 (R^2:0.995) and lowest MSE (MSE:0.0008) ratio.

1. Introduction

Since about two-thirds of the Earth's surface is covered with water, water is clearly one of the basic elements of human life [1]. In its purest form, it is odorless, colorless and tasteless. Due to the discharge of industrial waste into water, the level of pollutants in aquatic ecosystems has increased, which has led to an increase in the demand for water for domestic and industrial purposes. Water, which makes up 70 % of the Earth's surface, is undoubtedly the most valuable ordinary reserve on Earth. Living things on Earth could not exist without this invaluable solvent. Despite this, pollution of water resources occurs frequently. Hydrogen bonding and polarity are unique chemical properties that allow water to absorb, adsorb and dissolve a large number of compounds [2].

It is known that many major industries cause the presence of heavy metals in their wastewater. Industries are one of the largest users of water resources and producers of wastewater. The main industries responsible for wastewater generation are paint, textile, pharmaceutical, dye, pesticides, fertilizer, caustic soda, dairy, brewing, distilling, inorganic chemicals, asbestos, petroleum and other

* Corresponding author.
E-mail address: erdol@itu.edu.tr (N. Erdol-Aydin).

https://doi.org/10.1016/j.heliyon.2024.e39080
Received 22 August 2024; Received in revised form 4 October 2024; Accepted 7 October 2024
Available online 9 October 2024

engineering industries [3]. Heavy metals can be encountered at points where wastes from many different industries are discharged into water bodies. The Environmental Protection Agency (EPA) has listed zinc as a pollutant of concern, citing increasing cases of zinc poisoning. Electrolyte imbalance, abdominal pain and nausea, and muscle incoordination are the main signs and symptoms of zinc poisoning. Due to these potentially harmful effects, measures should be taken to reduce the presence of these pollutants to acceptable levels. The World Health Organization (WHO) has set the acceptable zinc content in drinking water as 5 mg/L [4,5]. Comprehensive assessment of water quality is a fundamental technical measure for the management and treatment of the aquatic environment [6].

A number of physical-chemical techniques can be used to treat wastewater containing heavy metals [7,8]. The most commonly used procedures are adsorption, membrane filtration, ion exchange, reverse osmosis and chemical precipitation, electrochemical processes, ozonation, hydrothermal treatment and stepwise extraction, biosorption coagulation-flocculation, phytoremediation and anaerobic membrane bioreactor [2,9–14]. In comparison, adsorption processes are superior to other techniques for wastewater recycling because they are cost effective, easier to design and operate, and are an effective process for removing zinc and other heavy metals from aqueous solutions [15]. Worldwide, activated carbon is the most common type of carbon used in wastewater treatment. Activated carbons are effective in removing heavy metals (i.e., lead, arsenic, mercury, and chromium) due to their non-biodegradability and environmental sustainability [16]. However, their use is limited due to their expensive nature. Therefore, a lot of research has been done to identify inexpensive and effective adsorbents. Various adsorbents such as fly ash, chitosan, cocoa and wheat hulls are used to remove zinc. Natural clay is considered as a suitable adsorbent because it is cheap and has a high removal efficiency [7,8]. Bentonite clays should receive much attention when used as natural adsorbents because they are cheap, effective and easy to store [17]. An important first step in the adsorption of certain pollutants by activated clay is the acidic activation of bentonite. This is called the “activation process”. The chemical and mineralogical properties of bentonite and its cation exchange capacity (CEC) change significantly with this process [17,18]. Temperature, treatment time and acid concentration are the main factors affecting the properties of acid-activated bentonite. Other factors are the type of activation agent used and the moisture level of the clay. Hydrogen ions replace the exchangeable ions in bentonite when treated with acid [17–19].

There are many studies on zinc removal from wastewater. Mellah and Chegrouche [20] used natural bentonite to adsorb zinc ions. In another study, zinc removal by Ca- and Na-bentonite was investigated [21]. Zn(II) was adsorbed on montmorillonite treated with sodium dodeacyl sulfate between 298 and 328 K by Lin and Juang [22]. Bayat compared the two to determine which Turkish fly ash could remove Zn(II) from an aqueous solution [23]. Rice bran was used for Zn(II) adsorption by Wang et al. [24]. Kanti and Gomez used natural bentonite to adsorb zinc from aqueous solution [25].

Artificial neural networks (ANN) are the preferred computational tools to model and predict various engineering problems involving many variables and parameters. ANN provides several advantages with its high learning capacity in the face of highly uncertain and complex input-output relationships. There are different ANN methods and architectures that can be used to model and calculate wastewater treatment process applications [14,26–28].

In this study, zinc in aqueous solutions was removed using bentonite as an adsorbent. Bentonite is an abundant, environmentally friendly, low-cost material that is quite useful for removing pollutants from water solutions due to its high adsorbent performance. These clays have not lost their importance from the past to the present due to the advantages they provide, on the contrary, studies on the subject have gained momentum. Bentonite based adsorbents can be used in the removal of organic and inorganic pollutants, radionuclides and other inorganic pollutants. It is possible to come across studies in the literature where different bentonite sources are used as adsorbents in the adsorption process [29–31].

Since bentonite sources are natural sources, they can be found in different contents and structures depending on the region where they are extracted, and their adsorption performance may also vary. For this reason, the bentonite used in this study, which belongs to the Ordu-Unye region in Turkey, has not been previously used for a similar purpose in the literature and examined as an adsorbent. When literature sources, especially in recent years, are examined, it is seen that the use of various bentonite sources in the adsorption of different pollutants still needs to be examined and investigated. This study also used a bentonite source not previously mentioned in the literature for zinc removal from wastewater and demonstrated its performance in detail. The effects of variables such as pH, contact time, adsorbent dose and initial zinc concentration on zinc removal through batch processes were investigated. Dubinin-Radushkevich (D-R), Freundlich, Temkin, BET and Langmuir isotherm models were used to study the equilibrium isotherms of batch systems. In addition to detailed parametric adsorption and isotherm studies, kinetic and thermodynamic studies were presented. Acid activation of bentonite upon adsorption was also carried out according to theoretical information found in the literature. The effects of activated bentonite on the adsorption capacity with two different acids, nitric and sulfuric acid, were compared.

In addition to all these experimental studies, this study also includes studies on computer learning for modeling and predicting the process with artificial neural networks using experimental results. Thus, the predictability of the process will increase, and more accurate results will be achieved with fewer experiments, less cost and time. There is still a lack of information in the literature on this type of studies that present both experimental data and studies conducted with ANN together. For this purpose, the most suitable method was determined based on high correlation (R^2) value and low minimum mean square error (MSE). In other words, as mentioned earlier, this study differs from the existing literature in that it simultaneously presents comprehensive ANN studies along with kinetic, isotherm and thermodynamic studies, in addition to a detailed examination of the effects of experimental parameters on zinc removal.

Table 1
Chemical composition of Ordu-Unye bentonite.

Chemical Grups	% Amounts
SiO_2	62.94 %
Al_2O_3	19.17 %
CaO	2.04 %
Fe_2O_3	2.71 %
MgO	3.88 %
TiO_2	0.18 %
Na_2O	0.80 %
K_2O	2.36 %
LECO Carbon	0.020 %
LECO Sulfur	0.008 %

2. Materials and methods

2.1. Materials

Zinc chloride ($ZnCl_2$, 98 %, Merck, Germany) dissolved in deionized water was used as the zinc source in the experiments. Sodium hydroxide (NaOH, 0.01 M, Merck, Germany) and nitric acid (HNO_3, 0.01 M, %65, Merck, Germany) were utilized to continue adjusting pH. The adsorbent was Ordu-Unye bentonite (one of the local mining companies in the region, Unye Madencilik, Turkey). The chemical compositions of Ordu-Unye bentonite is shown in Table 1. These data were obtained from the local producer of Ordu-Unye bentonite. The bentonite sample was kept at 100 °C for 2 h before using.

2.2. Acid modification

On account of evaluate the impact of activation conditions on zinc adsorption, the process was carried out a batch setup. For understanding the effect of acid type on activation process, nitric acid (65 wt%, Merck, Germany) and sulfuric acid (98 wt%, Merck, Germany) were used [17].

2.3. HNO_3 acid modification procedure

Dry bentonite powder which is 4 g and 200 mL HNO_3 (0.05 M) acid solution was mixed well into three-neck flask equipped with a condenser. Sample was activated at 98 °C for 60 min. The suspensions were mixed and heated during the activation using a magnetic stirring mixer. After being filtered, the activated sample was washed with distilled water multiple times and dried in an air oven at 100 °C for 24 h [17].

2.4. H_2SO_4 acid modification procedure

H_2SO_4 (200 mL, 0.25M) was mixed with 20 g of raw bentonite. The clay was heated to 97 °C in a shaking water bath for 6 h, with the fumes condensing by reflux, to activate the acid. After that, the sample of activated clay was repeatedly cleaned with distilled water to get rid of sulfate ions. Thereafter, the sample was kept on hold at 100 °C for 24 h at in the air oven [7].

2.5. Analyzes and characterizations

An instrument called the UV/vis spectrophotometer (Jenway, Model 6305,Japan) was used to analyze zinc. All adsorption tests were conducted using the shaker (Buhler, Germany), and the pH-meter (WTW Inolab pH 720, Germany) was utilized to alter pH.

The changes due to acid-activation were examined by BET-surface area characterization method (BET–Surface Area Analyzer Nova Model 1200, a single point method, USA), the Fourier transformed infrared (FTIR, PerkinElmer Frontier FTIR, USA) spectra and X-ray diffraction (XRD, Bruker 8D Advance diffractometer, Germany) analysis.

2.6. Adsorption experiments

Adsorption of zinc with Ordu-Unye bentonite was carried out with the batch process. 2.08 g of $ZnCI_2$ were dissolved in distilled water (1 L) to form 1000 mg/L of zinc solution. These stock solutions were diluted to prepare zinc solutions in certain concentrations. It was found that the samples had a 50 mL capacity. NaOH and HNO_3 were utilized to alter the pH. In the shaker, a temperature of 23 °C and a stirring rate of 250 rpm were applied. After the anticipated contact times, samples were taken from the medium, and filtered to separate the clay particles.

In the experiments, the initial and post-adsorption zinc ion concentrations were determined using the Zincon method (Standard Methods for the Examination of Water and Wastewater, APHA Method 3500-Zn, Zincon method) using a UV-spectrophotometer. In this method, zinc forms a blue complex with the Zincon indicator in a solution adjusted to pH 9.0. Zincon is one of the most commonly

Table 2
Effects of different pH values.

pH values	C_e (mg/L)	q_e (mg/g)	Efficiency (%)	Absolute error for LM	Absolute error for SCG	Absolute error for BR
3	1.25	12.19	97.50	0.17	1.44	0.09
4	1.25	12.19	97.50	0.49	1.33	0.96
5	1.61	12.10	96.78	0.74	0.54	0.83
6	1.61	12.10	96.78	1.24	0.50	0.90
7	1.61	12.10	96.78	0.16	0.44	0.58
8	1.81	12.05	96.40	0.19	0.11	0.09
9	1.91	12.01	96.08	0.02	0.90	0.06

used chelating agents in the determination of zinc ions. A spectroscopically analyzable complex is formed by the addition of cyanide, Zincon, and cyclohexanone to the medium, respectively. The absorbance values of the samples were measured for a wavelength of 620 nm [32,33]. In this study, the effect of initial concentration, amount of adsorbent, pH and contact time were investigated on zinc removal.

2.7. Adsorption models

Batch adsorption investigations were used to determine zinc equilibrium isotherms. Using Equation (1), the amount of adsorbed heavy metal (q_e) per unit mass of adsorbent was calculated:

$$q_e = \frac{(C_0 - C_e) \times V}{m} \tag{1}$$

where m is the bentonite mass (g), V is the solution volume (L), C_e is the concentration of pollutants at equilibrium (mg/L), and C_0 is the initial concentration of heavy metal [7]. The percentage of adsorbed metal relative to the initial concentration was used to express the adsorption efficiency (ɳ) as (Equation (2)):

$$\eta = \left(\frac{C_0 - C_e}{C_0}\right) \times 100 \tag{2}$$

These data were used in calculations, and adsorption curves were produced [5,34].

2.8. Modeling with artificial neural networks

Within the scope of this study, Matlab R2017b (The MathWorks) software was used to examine artificial neural networks models. In this context, feed-forward backpropagation network was chosen as the network type and "LEARNGDM" was chosen as the learning function. In order to select the most appropriate transfer functions for the hidden layer and output layer, the “LOGSIG”, “PURELIN” and “TANSIG” functions were changed and examined one by one. The function pair that gave the lowest MSE and the highest R^2 values were selected as the most appropriate, and the ongoing studies were continued with this function pair. The R^2 and MSE values mentioned here were calculated according to Equation (3) and Equation 4.The neural architecture included input, hidden and output layers. To decide the optimum number of neurons, the number of hidden neurons in the hidden layer was changed from 2 to 10. In ANN models, Levenberg–Marquardt (LM), Scaled Conjugated Gradient (SCG) and Bayesian Regularization (BR) training methods were used. In all these studies, random division of data was preferred. Before the data was used in calculations in the ANN, it was normalized to a value between 0 and 1 to reduce the impact of outliers and facilitate learning.

$$R^2 = \sqrt{\frac{\sum_{i=1}^{n}(Yi - \overline{Y}i)^2 - \sum_{i=1}^{n}(Yi - \overline{\widehat{Y}}i)^2}{\sum_{i=1}^{n}(Yi - \overline{Y}i)^2}} \tag{3}$$

$$MSE = \frac{1}{n}\sum_{i=1}^{n}\left((Yi - \widehat{Y}i)^2\right. \tag{4}$$

In Equations (3) and (4), n is the observation numbers, Yi is the percentage of adsorbed zinc to the initial amount, $\overline{Y}i$ is the average zinc removal percentage, and $\hat{Y}$i is the percentage of zinc to the initial amount predicted by the model [26–28].

3. Results and discussion

3.1. Effect of pH

Ambient pH is a parameter known to have an effect on the ionization degree, the chemistry of metal ions and the surface properties of the mineral. Ordu-Unye bentonite was used to adsorb zinc, and metal solutions with a volume of 50 mL and a concentration of 50

Table 3
Effects of clay dosage on efficiency.

Adsorbent dosage (g)	C_e(mg/L)	q_e (mg/g)	Efficiency (%)	Absolute error for LM	Absolute error for SCG	Absolute error for BR
0.01	33.87	80.66	32.26	1.09	3.19	1.30
0.03	26.20	39.67	47.60	5.76	5.20	3.88
0.05	26.03	23.97	47.94	4.37	6.37	5.74
0.10	10.38	19.81	79.23	4.26	3.07	4.14
0.20	2.77	11.81	94.46	1.31	1.05	0.83
0.30	2.77	7.87	94.46	0.40	2.42	0.58
1.00	2.77	2.36	94.46	0.05	2.70	0.04

mg/L were employed, with pH values ranging from 3 to 9. The trials maintained a consistent clay content of 0.2 g and determined that the agitation period should be 2 h at 250 rpm. Table 2 presents the results of this study.

When zinc was adsorbed onto natural clay, the greatest removal efficiency was achieved at pH 3 and pH 4, respectively. The adsorption efficiency was decreased a little bit with increasing pH values but nearly constant until 7. However after pH 8, it started to decrease a little.

Silicon-oxide and aluminum-oxide in the structure of bentonite turn into silanol (Si-OH) or aluminol (Al-OH) form when bentonite is thrown into water. It is known that in a highly acidic environment (pH < 3), silanol (Si-OH) or aluminol (Al-OH) transforms into Si-OH^{2+} and Al-OH^{2+} forms, causing the mineral surface to become positively charged. In this case, electrostatic repulsion occurs between the heavy metal and the adsorbent surface and adsorption becomes difficult. According to a study conducted by Mekhamer [35], the point of zero charge (PZC) value of raw bentonite was reported to be pH 3. It is known that the surface charge of bentonite is positive below this value. At pH values above this value, the negative charge of the surface increases with increasing pH [35]. For this reason, pH experiments started from pH 3. As the pH increases, silanol (Si-OH) or aluminol (Al-OH) begins to transform into Si-$(OH)^{2-}$ and Al-$(OH)^{2-}$ forms. Thus, the positive charge of the surface decreases and it begins to become negatively charged. Accordingly, the zinc ion and bentonite mineral interaction increases. As can be seen from the results, a plateau was reached between pH 3 and 7 and no significant change in adsorption behavior was observed in this range. This situation has also been reported in different studies [35–39]. On the other hand, it is known that after a certain pH value (pH > 7), the solubility of heavy metals decreases and hydroxyl compounds form and precipitate occurs. This inhibition of the adsorption mechanism explains the decrease in zinc sorption efficiency after pH 7 seen in the results [25,36].

In summary, the adsorption properties of bentonites can be explained by dissolution, ion exchange/adsorption and precipitation mechanisms. In fact, pH determines which of these mechanisms dominates the adsorption process. Due to the involvement of different mechanisms, it has been stated that the adsorption efficiency does not exhibit much change, similar to many studies in the literature [36,39,40]. Another reason for this is thought to be the adsorption time. In a study conducted by K. Bellir et al. [39], where the adsorption of zinc onto bentonite was examined, it was shown that the pH effect decreased with time. They reported that the pH effect disappeared especially after the 90th minute. In this study, similar to K. Bellir's study, since the pH effect was examined at the end of 120 min, no significant change was observed at different pH values.

3.2. Effect of adsorbent dosage

In order to find out the efficient dosage of adsorbent, different bentonite dosages varied between 0.01 and 1 were tried. Initial metal concentration was adjusted to 50 mg/L and pH value was kept 5. After addition of different amounts of adsorbent to solutions, experiment was carried out for 2 h. The results are listed in Table 3.

In Tables 3 and it is understood that the performance increases with increasing adsorbent amounts up 0.2 then there was no increase in adsorption. Because, in the same solution volume, there are more active sites due to the increase in the adsorbent amount. However, it can be seen that the amount of zinc adsorbed per unit adsorbent (mg/g mineral) decreased in this study as reported in the literature studies [25,37,41].

At high dosages, when the available metal concentration is not sufficient to completely cover the active sites on the adsorbent, low metal adsorption usually occurs. Furthermore, a poor specific removal may be the outcome of binding site interference brought on by an increased adsorbent dose. When the adsorbent amount increases, the interactions between the adsorbent particles become more significant and may result in physical obstruction of some adsorption sites, lowering the removal effectiveness. The electrically charged surface may produce electrostatic interferences as a result of these interactions, which reduces the attraction between the surfaces of individual particles and adsorbed solutes. At the same time, if the adsorption of metal ions is reversible, desorption is expected. Metal ions in the medium can be adsorbed at low adsorbent concentrations not only on the sorbent's surface but also within its interior, facilitating the metal ion concentration gradient. Consequently, when the amount of adsorbent is increased while maintaining a certain volume, the effective surface area decreases and less space is available per unit adsorbent mass [29,42].

A similar pattern of different adsorbent effects on metal ion removal has also been documented by a number of other researchers [36]. In the literatüre, it has been stated that lower adsorbent amount results in higher adsorption performance due to the increase in the solid/liquid interface area. It is said that the equilibrium adsorption capacity decreases for a given initial metal concentration as the concentration of the mineral in the solution increases and approaches a critical value at where all ions are adsorbed to the mineral [29,36,42,43].

Briefly, the results in Table 3 show that as the adsorbent amount increases, the adsorbed amount per unit adsorbent decreases and

Table 4
Contact time effect on adsorption efficiency.

Contact time (min)	C_e (mg/L)	q_e (mg/g)	Adsorption efficiency (%)	Absolute error for LM	Absolute error for SCG	Absolute error for BR
15	2.5	11.88	95.00	0.09	0.42	0.27
30	2.5	11.88	95.00	3.13	0.56	0.39
45	2.5	11.88	95.00	0.33	1.09	0.77
60	2.1	11.98	95.80	0.24	0.44	0.15
90	2.1	11.98	95.80	0.01	0.21	0.10
120	2.1	11.98	95.80	0.03	2.39	0.51

Table 5
The results of different metal concentration.

C_0 (mg/L)	C_e (mg/L)	q_e (mg/g)	Efficiency (%)	Absolute error for LM	Absolute error for SCG	Absolute error for BR
10	0.28	2.43	97.20	1.19	0.02	0.77
25	1.00	6.00	96.00	0.54	0.97	0.90
50	2.50	11.88	95.00	1.04	1.24	0.95
100	10.00	22.50	90.00	3.27	0.22	3.38
125	25.00	25.00	80.00	0.06	0.54	1.05
150	45.60	26.10	69.60	3.64	0.92	1.09
200	84.40	28.90	57.80	0.03	0.02	0.27

conversely, the removal performance percentage increases. This situation is similar to the results observed in previous adsorption studies. In studies conducted on the removal of zinc or similarly different cations [36,40,44,45], it has been reported that the adsorbed amount per unit adsorbent decreases with the increase in the adsorbent amount, which is consistent with the present study. In addition, in a study conducted on zinc removal [25], it was observed that the increase in the adsorbent amount improved the zinc removal percentage until a certain adsorbent amount was reached, similar to the present study.

Since there is no increase in adsorption efficiency when the quantity of adsorbent is increased beyond 0.2 g, this value was determined as the optimum amount of adsorbent for zinc removal.

3.3. Effect of contact time

The contact time was also one of the most important factor on the efficiency. In order to analyze the effect of contact time on zinc removal, samples were taken at different time periods varying between 15 and 120 min. Experiment was studied at pH 5 by using 0.2 g bentonite which was determinated previous work, and initial concentration was kept 50 mg/L. Table 4 displays the results.

As can be clearly seen from the results in Table 4, the adsorption process of zinc on the bentonite used in this study was very fast, and the adsorption efficiency reached 95 % even after 15 min. After this rapid increase, adsorption slowed down and at the end of 60 min, the adsorption process reached equilibrium with an efficiency of 95.80 %. As a result of this study, 60 min was selected as the optimum contact time. There are studies in the literature where adsorption equilibrium was reached quickly, as in this study [38, 45–47].

In a study involving the adsorption of zinc removal using Ca-Bentonite, it was determined that zinc was initially adsorbed very quickly on bentonite and then reached an equilibrium over time [46]. According to a different study showing the adsorption of zinc on illite, the process started quite fast and slowed down for 60 min until equilibrium was reached [47]. Similar to other studies, a study examining the adsorption of zinc on natural clay concluded that zinc reached its maximum adsorption efficiency after 5 min [38,45].

3.4. Effect of initial concentration

To determine metal concentration which varied from 10 to 200 mg/L effects on adsorption efficiency, experiment was carried out using 0.2 g bentonite for 60 min at pH 5. Results are given in Table 5.

It is known that adsorption is independent of initial concentration due to the low ratio of metal cations to adsorbent mass at low initial metal concentrations. More metal ions become accessible when the initial concentration is increased, and more metal ions are adsorbed for a given amount adsorbent. The motivation to overcome the mass transfer resistance and allow the metals to migrate from the massive solution to the mineral surface increases with higher initial concentrations of metal ions. However, as more metal cations are added per unit mass of adsorbent, the sites are gradually filled until saturation is reached. Several studies have also documented that increasing the initial concentration leads to an improvement in the adsorption capacity on the one hand and a decrease in the adsorption efficiency on the other hand [17,36,45]. In this study, an increase in adsorption capacity was observed, consistent with the studies mentioned in the literature. This increase increased rapidly up to 100 mg/L, but a slowdown was noted after this value.

On the other hand, as can be seen from Table 5, the adsorption efficiency remained high as the metal ion concentration increased, but started to decrease after 100 mg/L. It was concluded that the adsorbent reached saturation in the concentration range of 50 mg/L and 100 mg/L. Since the adsorbent, which is saturated after 100 mg/L, does not have enough area to adsorb the zinc ion, increasing zinc concentration decreased the adsorption efficiency. Different studies with a similar trend to the effect of initial concentration in this

Table 6
Adsorption isotherm models and fitting parameters for the adsorption of Zn ions on raw bentonite.

Models	Linearized Form of Equations	Values of the model parameters
Langmuir [24–26]	$q_e = Q_0\ (b \times C_e)/(1 + b \times C_e)$	Q_0 : 25.51 R^2 : 0.99 b: 0.37
Freundlich [24,25]	$\text{Log } q_e = \log K_f + (1/n)^* \log C_e$	Kf: 5.97 R^2 : 0.90 n: 2.33
D-R [26,27]	$\text{Ln } q_e = \text{Ln } q_m - Be^2$	B: 0.0016 R^2 : 0.81 q_m: 20.07
Temkin [28]	$q_e = B \ln K_t + B \text{ Ln } C_e$	B: 4.97 R^2 : 0.97 K_t: 5,01
BET [5]	$Ce/[q_e \times (C_0 - C_e)] = 1/(q_m k) + (C_e/C_0) \times [(k-1)/(q_m k)]$	q_m: 21.05 R^2 : 0.77 k: 10.80

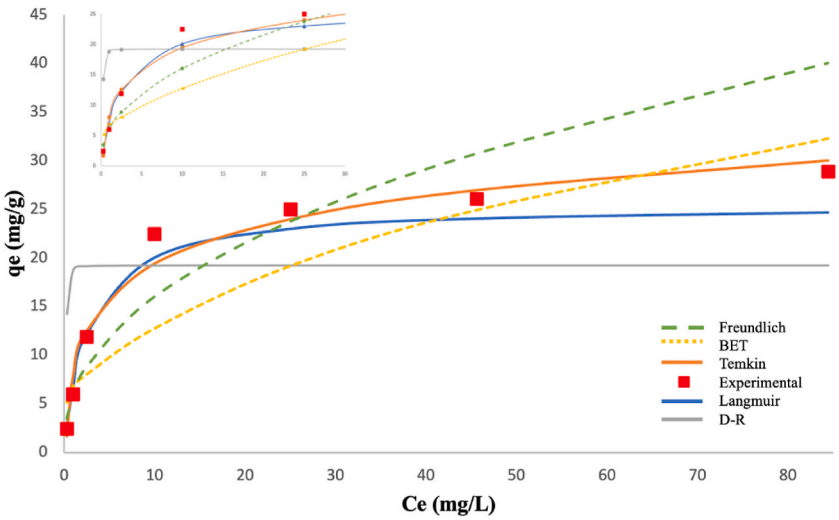

Fig. 1. Adsorption isotherm models.

Table 7
A comparison of maximum adsorption capacity for Langmuir model of previous studies in literature.

Material	Adsorption capacity (mg/g)	Reference
Natural zeolite	3,45	[21]
Natural bentonite	15,46	[5]
β-cyclodextrin-modified pectin	9213	[48]
Natural bentonite	24	[36]
Chitosan/cellulose	19,81	[49]
Durian tree sawdust (	22,78	[50]
Coconut coir	24,39	[50]
Fruit bunch	21,19	[50]
Bentonite	21,09	[51]
Paddy husk biochar	26,53	[52]
Chicken manure	11,12	[53]
Ca-alginate-biochar	120	[54]
commercial activated carbon	14	[55]
Ordu-Unye bentonite	25,51	In this work

study can also be found in the literature [36,45]. In the study conducted by Kaya et al. [36], an investigation was made between 1 and 200 mg/L metal concentrations. While an increase in adsorption capacity was observed with increasing initial concentration at the beginning, it was reported that it did not show much change after 60 mg/L. In addition, in the studies conducted by Veli et al. [45] at 20–160 mg/L metal concentrations, the optimum metal concentration was found to be 100 mg/L.

Table 8
Kinetic model equations and parameters.

Models	Equations	Parameters	
Pseudo first order		qe(cal.)	0.1735 mg/g
	$\log(q_e - q_t) = \log(q_e) - \frac{k_1 \times t}{2.303}$	k_1	0.02 1/min
		R^2	0.7059
Pseudo second order		qe(cal.)	12.0048 mg/g
	$\frac{t}{q_t} = \left(\frac{1}{q_e}\right) \times t + \frac{1}{k_2 \times q_e^2}$	k_2	0.303 mg/gmin
		R^2	>0.99
Intraparticle diffusion		k_3	0.018 mg/gmin$^{1/2}$
	$q_t = k_3\sqrt{t} + I$	I	11.797 mg/g
		R^2	0.7271
Experimental Data		qe(exp.)	12 mg/g

Table 9
Results of acid activated and raw bentonite comparatively.

Adsorbent	C_e (mg/L)	q_e (mg/g)	Adsorption efficiency (%)	pH value after experiment
Raw bentonite	2.50	11.88	95.00	8.10
HNO_3 activated bentonite	20.80	7.30	58.40	3.24
H_2SO_4 activated bentonite	28.10	5.47	43.80	3.35

3.5. Comparison of adsorption isotherms

Adsorption behaviours of bentonites for zinc ion were described with the Langmuir, Freundlich, D-R, Temkin and BET models. The model parameters values were determined by equations which are in Table 6 [7].

According to correlation coefficient, it can be said that Langmuir and Temkin isotherm models are very well to explain study results. In addition, isotherm coefficients and experimental C_e values were used for calculating theoretical q_e values. Fig. 1 was obtained using by theoretical q_e and experimental C_e values. It is clearly seen in Fig. 1, Temkin and experiment values correspond to each other. Based on this, it can be interpreted that the adsorption of zinc on bentonite occurs on heterogeneous surfaces, the bond between the metal ion and the adsorbent is strong, and it interacts with the functional groups where adsorption occurs in a very short time.

When the maximum adsorption capacity of the adsorbent used in this study obtained from the Langmuir isotherm model is compared with the maximum adsorption capacity of other adsorbent materials previously reported in the literature (Table 7), it is seen that the bentonite from Ordu-Unye region used in the present study has higher and comparable capacity in many cases. The bentonite adsorbent used in the present study is a natural product, abundant in nature, effective high surface area and good performance in zinc removal have led to this bentonite source being considered as a sustainable and economical adsorbent source.

3.6. Adsorption kinetics

Pseudo first order, pseudo second order and intraparticle diffusion models were tested to determine the zinc adsorption kinetics of bentonite. These experiments were carried out by measuring samples taken from the medium at pH 5 at an initial concentration of 50 mg/L at time intervals ranging from 15 to 120 min. The equations of the models and the results of the parameters of the models are summarized in Table 8 k_1, k_2 and k_3 in the table represent the pseudo first order, pseudo second order and intraparticle diffusion coefficients, respectively [56,57]. q_e and q_t represent the amount of zinc adsorbed in the equilibrium and at any time, and t represents the time.

When all three models are examined, it is seen that the most suitable kinetic model for the adsorption process is the pseudo second order. The q_e values calculated using this model (12.0048 mg/g) and the experimental (12 mg/g) are very close to each other. In addition, the R^2 of the model is > 0.99, and k_2 is 0.303 mg/gmin. It is seen that the R^2 value for the pseudo first order is quite low. This means that the model will be insufficient to explain the kinetic data related to this process. Finally, it can be concluded that the Intraparticle diffusion model is also not suitable to explain the kinetic data related to this adsorption process with the R^2 value of 0.7271.

3.7. Acid activated bentonite effect on adsorption capacity

Since there are few sources in the literature on the zinc adsorption of acid modification, the effect of different acids on the adsorption of zinc on bentonite was examined in this study.

Bentonite was activated with HNO_3 and H_2SO_4 to examine the effect of the acid modification of the bentonite on adsoption capacity. Results are shown in Table 9. In the experiments, adsorbent amount, initial concentration and contact time were taken as 0.2 g,

Table 10
Specific surface area of raw and acid activated bentonites.

Adsorbents	Specific Surface Area (m^2/g)
Raw bentonite	64.56
HNO_3 activated bentonite	69.16
H_2SO_4 activated bentonite	83.91

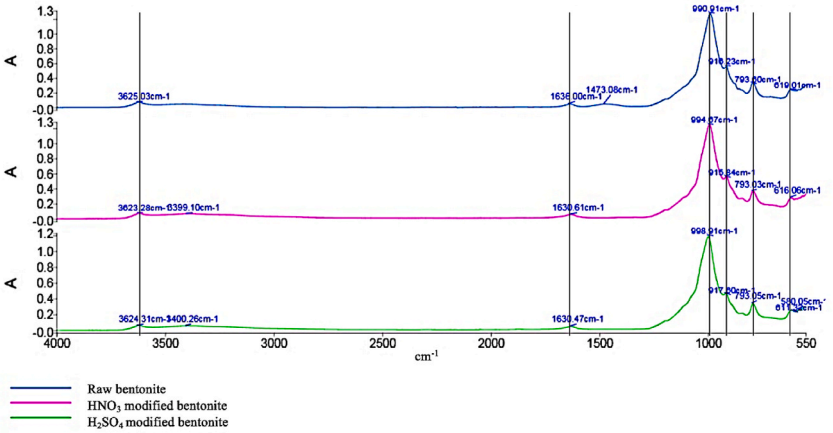

Fig. 2. FTIR analysis of raw and acid activated bentonites.

50 mg/L and 60 min, respectively.

Bentonite can be divided into 3 classes according to pore sizes: microporous, mesoporous and macroporous. Adsorption considerably are related to presence of micropres and mesopores [17].

Impurities on bentonite dissolves in acidic media and also the exchangeable cations replaces with hydrogen ions. Therefore the surface area of clay generally increases. Rising of the surface area and changing in pore structure of clay are related with chemical composition of clay, types of exchangeable cations, presence of the other mineral types in clay, type of acid and acid concentration, treating temperature and time of acidification of the clay [17].

The surface area of raw and acid activated bentonites were determinated and results are in Table 10. As seen from the results, the surface area of bentonite activated with sulfuric acid was found to be higher than other bentonite types.

Fig. 2 displays the FTIR spectra of both acid-modified and raw bentonite. The O-H stretching vibration of bound water and the O-H stretching vibration of Al-OH groups are responsible for the peak at 3620 cm^{-1} observed in the FTIR spectra of raw bentonite and acid modified bentonites. The peak located approximately at 1630 cm^{-1} is attributed to the water molecules' O–H bonds bending within the silicate matrix. Stretching vibrations of Al-O, Al-Al-OH, and Si-O functional groups produce the peak values at 793 cm^{-1}, 918 cm^{-1}, and 990 cm^{-1}, respectively. Furthermore, the peaks at 793 cm^{-1} point to the quartz's presence in bentonite. The bands at 617 cm^{-1} indicate the Al-O-Si-O bond (presence of feldspar). The presence of similar peaks in all three spectra is interpreted as no change in the mineralogical structure of bentonite [58–60].

The compositions of the bentonites were investigated by XRD and the results were given in Fig. 3. It is said that impurities like calcite and quartz dissolved by acid activation. However montmorillonite minerals are nearly similar in raw and acid activated bentonites.

It is possible to come across studies in the literature examining the effect of acid treatment on adsorption [61,62]. In these studies, it is seen that the effect of acid activation can vary depending on the ionic form of the material to be adsorbed. The common opinion in the studies is that acid treatment causes the adsorbent surface to become neutral or even positively charged. Depending on the situation of the adsorbent surface, adsorption can be affected positively or negatively depending on the ionic form of the substance to be adsorbed in that environmental conditions. The adsorption of zinc and cadmium from aqueous solutions on both natural and activated bentonite was investigated by Pradas et al. They showed that modification of bentonite by acid treatment reduced the adsorption capacity. Moreover, further decrease in the adsorption capacity was reported when the molarity of the treated acid is stronger [61].

Similar to the studies in the literature mentioned above, in this study, as clearly seen in Fig. 4, raw bentonite has the highest adsorption capacity compared to acid modified bentonites. This can be explained by the neutralization and even positive charging of most functional groups on the bentonite surface due to acid activation. Therefore, the interaction between bentonite and zinc ions decreased significantly. Based on the knowledge that clay minerals affect the pH of the environment [43,63], the pH values measured after the experiment also prove this fact.

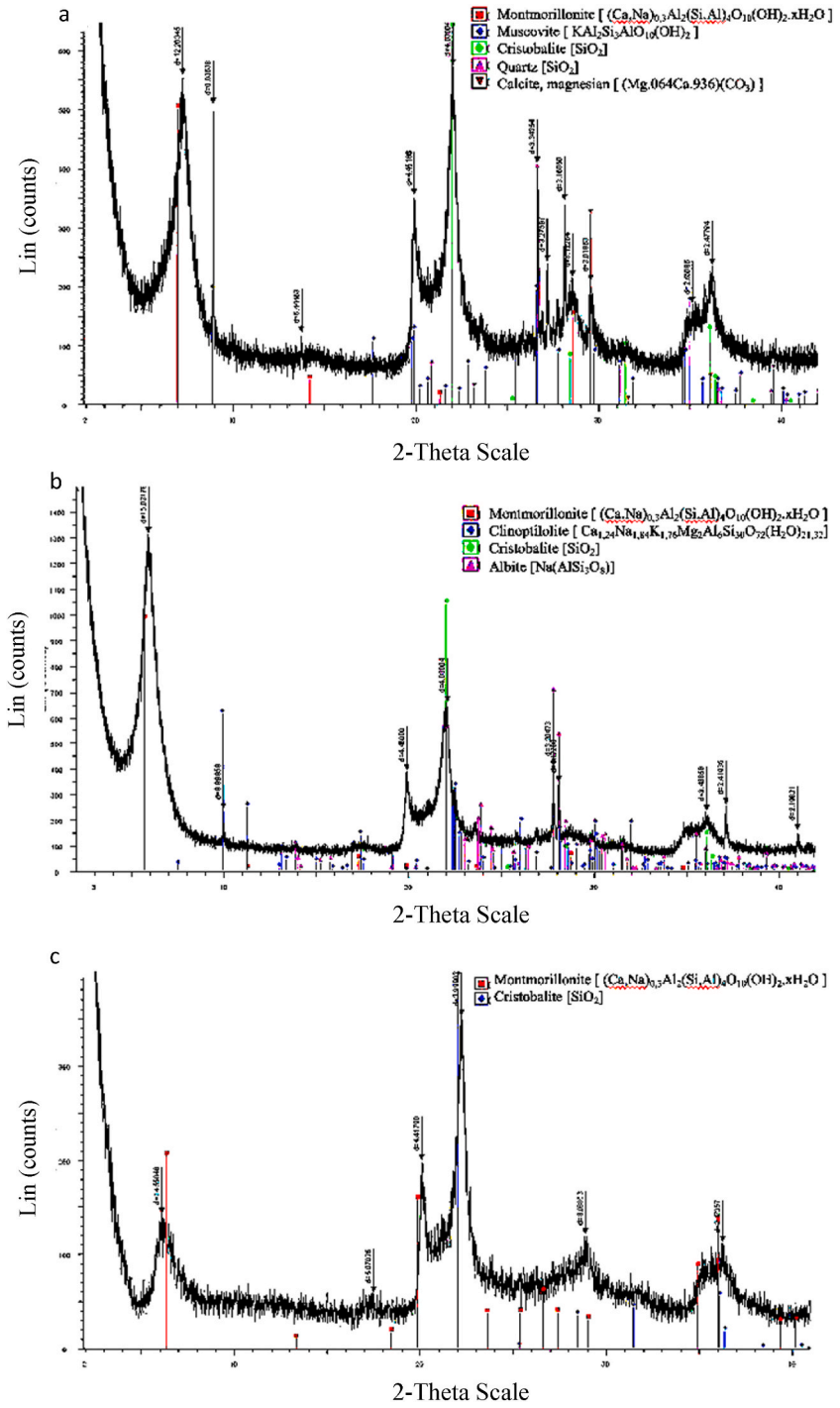

Fig. 3. XRD analysis of, a) raw bentonite, b) H_2SO_4 modified bentonite, c) HNO_3 modified bentonite.

3.8. Thermodynamic studies

Thermodynamic parameters are key factors for understanding the entropy and energy changes through processes. The changes in enthalpy (ΔH°) and entropy (ΔS°) were determined from linear plots of log (q_e/C_e) vs 1/T (Fig. 5) using the following equations:

$$K_c = q_e/C_e \quad (5)$$

$$\text{Log } (q_e/C_e) = -\ \Delta H^\circ\ /\ 2.303\ RT + \Delta S^\circ\ /\ 2.303\ R \quad (6)$$

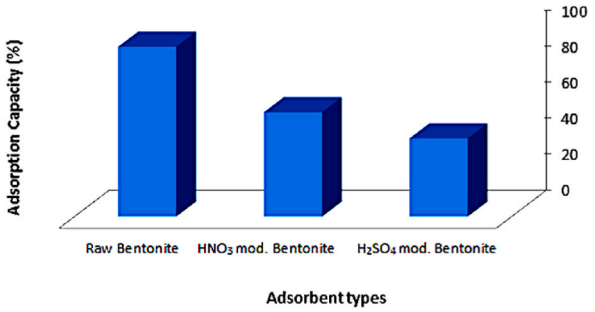

Fig. 4. Effects of acid activation on adsorption capacity.

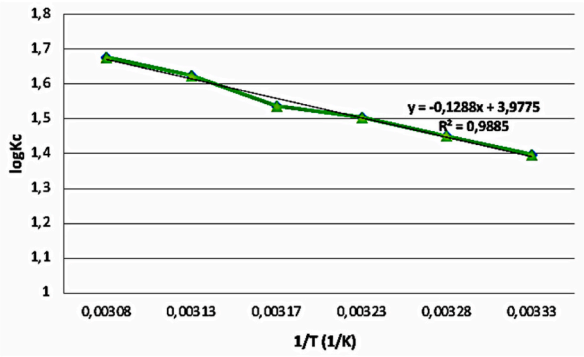

Fig. 5. Thermodynamic plot for adsorption of zinc ions onto bentonite.

Table 11
Thermodynamic parameters.

T(°C)	ΔG°(kJ/mol)	ΔH°(kJ/mol)	ΔS°(kJ/molK)
27	−8.02	33.07	0.326
32	−8.47		
37	−8.92		
42	−9.27		
47	−9.95		
52	−10.43		

Table 12
The R^2 and MSE results for different models.

Models	Activation Functions	LM		BR		SCG	
		R^2	MSE	R^2	MSE	R^2	MSE
1	logsig-logsig	0.9	0.0025	0.6952	0.0708	0.51568	0.0178
2	logsig-purelin	0.76	0.0045	0.98552	0.0008	0.63311	0.0078
3	logsig-tansig	0.99	0.001	0.6867	0.0682	0.95785	0.0026
4	purelin-logsig	0.95	0.0178	0.64232	0.0872	0.84793	0.0961
5	purelin-purelin	0.48	0.0013	0.74309	0.0364	0.7438	0.0169
6	purelin-tansig	0.91	0.0006	0.9609	0.0198	0.274	0.135
7	tansig-logsig	0.94	0.0008	0.668	0.0723	0.94047	0.0825
8	tansig-purelin	0.99	0.0019	0.99182	0.0005	0.97476	0.0001
9	tansig-tansig	0.96	0.0063	0.96826	0.0009	0.96503	0.0093

The free energy change (ΔG°) was cakculated using the following equation:

$$\Delta G^\circ = \Delta H^\circ - T\,\Delta S^\circ \quad (7)$$

The values of ΔG° obtained at 27, 32, 37, 42, 47, and 52 °C are −8.02,-8.47, −8.92, −9.27, −9.95, and −10.43 kj/mol, respectively. Obtaining negative ΔG° values is a sign of spontaneous adsorption process [64]. For this reason, the increase in -ΔG° values with

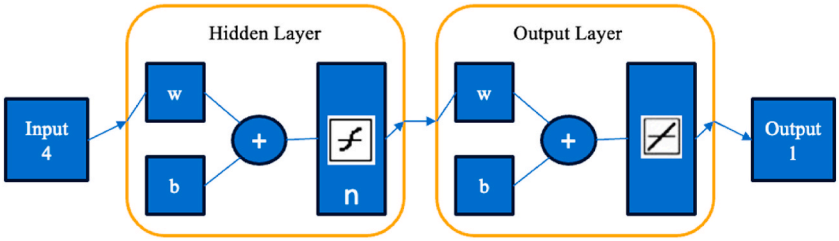

Fig. 6. ANN architecture.

Table 13
The R^2 and MSE results for different neuron numbers of different training methods.

Number of Neurons	BR		SCG		LM	
	R^2	MSE	R^2	MSE	R^2	MSE
2	0.9791	0.0008	0.51573	0.0041	0.9439	0.0053
3	0.9857	0.0008	0.9313	0.0013	0.6528	0.082
4	0.99529	0.0008	0.1639	0.0384	0.9904	0.0125
5	0.99433	0.0008	0.99322	0.0002	0.9275	0.0037
6	0.995	0.0008	0.8011	0.0187	0.9898	0.0005
7	0.9947	0.0008	0.8321	0.0383	0.7302	0.0235
8	0.9115	0.0004	0.457	0.0206	0.9424	0.0006
9	0.98919	0.0009	0.8974	0.0059	0.6382	0.0082
10	0.99382	0.0007	0.8752	0.04137	0.9948	0.0008

increasing temperature can be interpreted as adsorption being more suitable at a higher temperature. A positive ΔH° value (33.07 kj/mol) could be interpreted as an endothermic adsorption process [64,65]. A ΔH° value below 40 kj/mol indicated zinc physisorption onto bentonite structure [66,67]. Additionally, positive value of ΔS° (0.326 kj/molK) qualifies as an indicator of randomness. The reason for this may be that displaced water molecules gain more translational entropy than metal ions lose during the adsorption [68]. A summary of the thermodynamic parameters is presented in Table 11.

3.9. Artificial neural network (ANN)

Studies were carried out on three different models: Levenberg–Marquardt (LM), Scaled Conjugate Gradient (SCG) and Bayesian Regularization (BR) training methods [28]. Determining the optimum ANN architecture started by deciding what the most appropriate transfer functions were for the hidden and output layers. Table 12 shows the R^2 and MSE values obtained by changing the "LOGSIG", "PURELIN" and "TANSIG" functions for both layers one by one for all 3 training methods. The number of hidden neurons for each model here is kept constant at 6. As can be clearly seen from the results, Model 8 in the table (TANSIG-PURELIN model) has the highest R^2 and lowest MSE value for all 3 training methods. For this reason, it was decided to continue with this dual function group in determining the best training method. Fig. 6 shows the proposed network structure.

To determine the best training method, ANN architecture for all 3 training methods was created. In all 3 methods, the number of neurons in the hidden layer was changed between 2 and 10 and MSE and R^2 values were determined for all of them. Table 13 shows R^2 and MSE values for different numbers of hidden nodes for each training method. It is known that the model should have high R^2 and low MSE values when deciding on its predictive accuracy [14,28,69,70]. Accordingly, the best result (MSE: 0.0008, R^2: 0.9948) in the network optimized with the LM method was achieved when 10 hidden nodes were used. At the same time, the best result (MSE: 0.0002, R^2: 0.99322) of the network using the SCG training method was seen when 5 hidden neurons were used. In addition, in studies conducted with BR training method, the best result (MSE: 0.0008, R^2: 0.99529) was found when 4 hidden neurons were used.

The graphs of ANN data for training, validation, testing and all cases where the best results are obtained for all 3 training methods are shown in Fig. 7. In Fig. 7a, the R^2 values of the network optimized according to the LM training method for training, validation, testing and the entire data set in the best condition are 0.99364, 0.99793, 0.97606 and 0.99485, respectively, and the MSE value of the best performance was seen 0.00079571.

The R^2 values and MSE value in the best condition of the network trained according to the SCG method are shown in Fig. 7b. Here, the R^2 values calculated for training, validation, testing and the all data set were 0.99112, 0.99998, 0.98108 and 0.99322, respectively, and the MSE value of the best performance was found to be 0.00023854.

Finally, in Fig. 7c, the R^2 value of the network trained according to the BR method is 0,99323 for training, R^2 value for testing is 0.99983 and R^2 value for all data is 0.99529. In addition, the MSE value of this network under best conditions is 0.00077387. In the network trained with the BR method, the R^2 value is not calculated for validation due to its own algorithm [28].

In summary; the architecture of the optimized network was determined as 4:10:1, 4:5:1 and 4:4:1 for the three training methods LM, SCG and BR, respectively. The results of the ANN analysis performed are important in terms of making the process predictable with

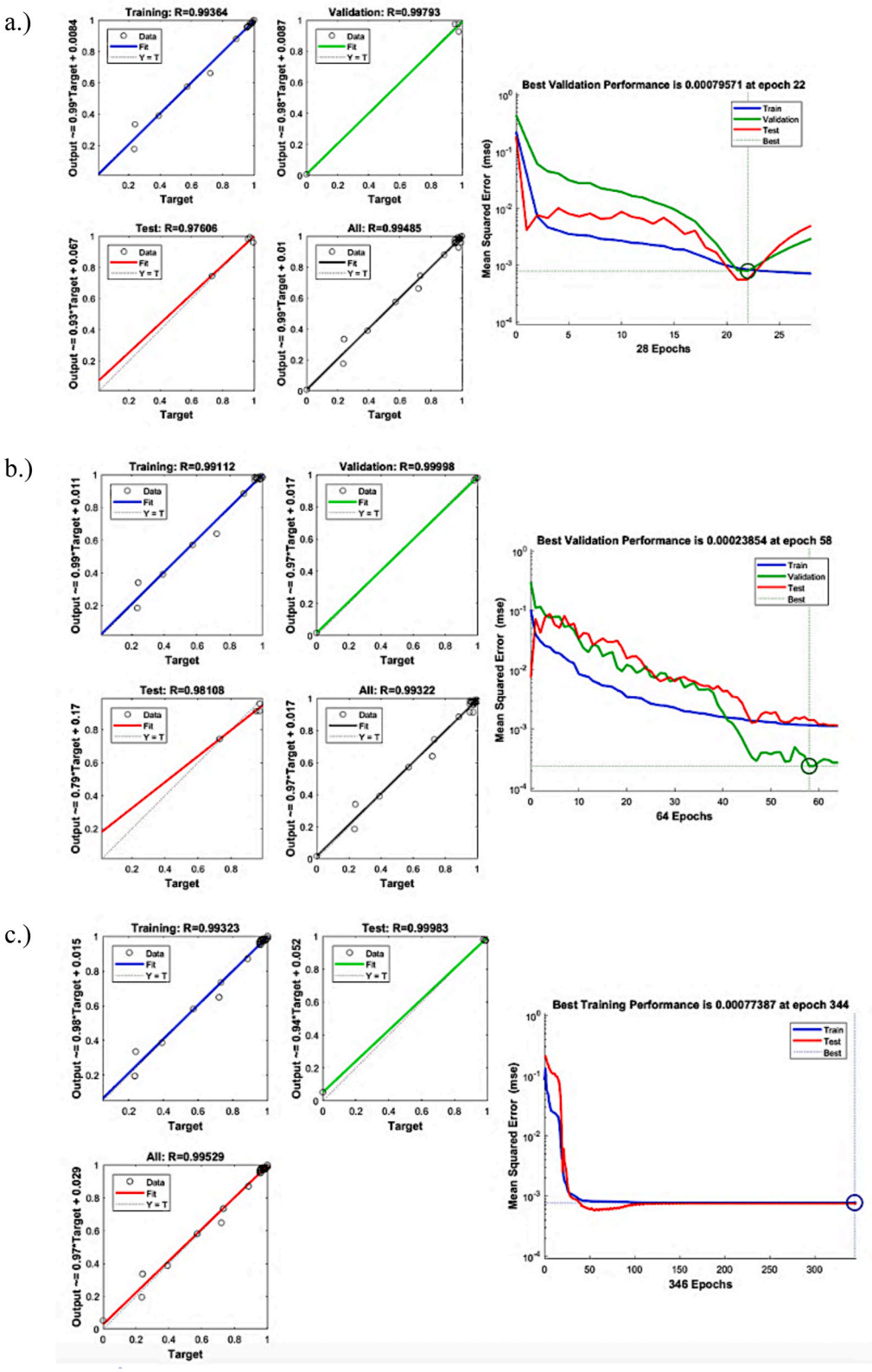

Fig. 7. R^2 value for training, testing, validation and all data sets and MSE value for the best architecture of optimized ANN model with a) Levenberg–Marquardt training method, b) Scaled Conjugate Gradient training method and, c) Bayesian Regularization training methods.

Table 14
Some experimental results and estimated results from the three models.

Efficiency (%)			
Experimental	LM	SCG	BR
97.50	97.67	96.06	97.59
96.40	96.59	96.51	96.49
32.26	31.17	29.07	33.56
47.94	52.31	54.31	53.68
79.23	74.97	76.16	75.09
94.46	94.51	97.16	94.42
95.00	91.87	95.56	95.39
96.00	96.54	96.97	96.90
90.00	86.73	89.78	86.62
80.00	80.06	80.54	78.95
69.60	73.24	68.68	70.69
57.80	57.77	57.82	57.53

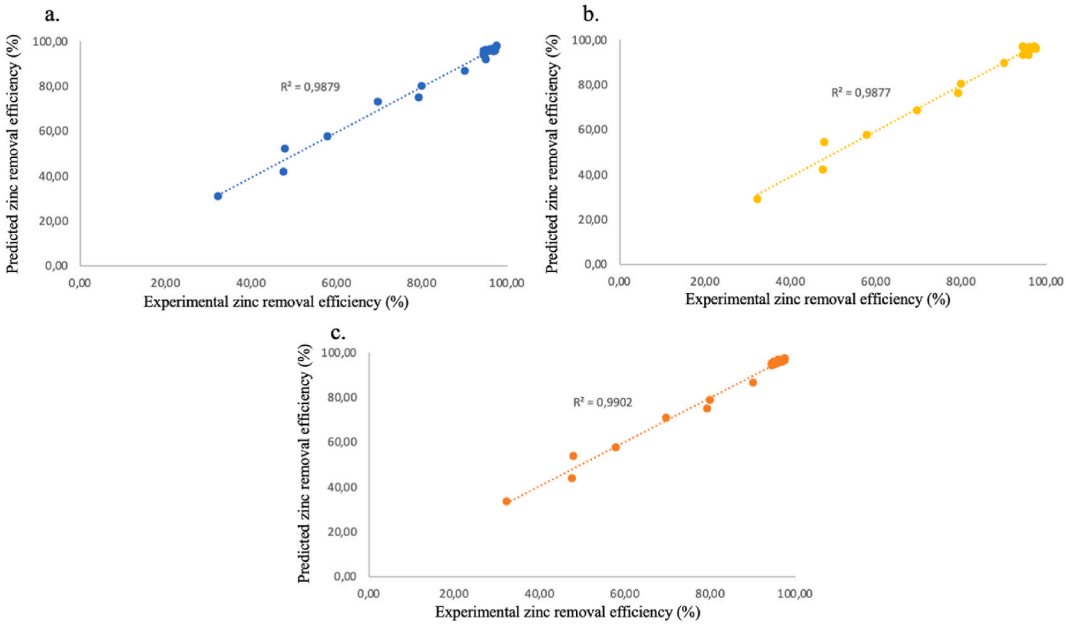

Fig. 8. Comparison between the experimental data and predicted values of zinc removal efficiency (%) using a.) LM model, b.) SCG model, c.) BR model.

the help of the models obtained in this way and, accordingly, making decisions about the process without the need for a large number of experiments. In order to evaluate the usability of the obtained models, the some experimental results and the predicted results according to the three training methods are given in Table 14 for comparison. As can be clearly seen from the results in the table, it was seen that the mentioned models predicted the experimental results with high accuracy. In other words, it was determined that the models represented the adsorption process well. Thus, it is possible to make preliminary predictions for different conditions and evaluate the process without conducting too many experiments.

Fig. 8 shows the comparison between the experimental data of zinc removal efficiency (%) with bentonite for the best conditions of all three tested models and the values estimated by the models. Here, it is seen that the R^2 values of each selected model are quite high and close to each other. This is thought to indicate that these three models with different optimum architectures exhibit high compliance with the experimental data [71,72].

4. Conclusions

In this study, the zinc adsorption performance of Ordu-Unye bentonite was examined in detail for different adsorption conditions. Here, the best result, 97.5 % efficiency, was achieved under the conditions of pH 3, 0.2 g adsorbent amount, 50 mg/L initial concentration, and 120 min. As a result of the investigations, it was revealed that the adsorption efficiency was significantly affected by the changes in the initial concentration of zinc and the amount of adsorbent (compared to pH and contact time parameters). Studies were

carried out on adsorption isotherms and it was found that the most suitable isotherm models for the process were Langmuir and Temkin. It was also determined that the adsorption process was a physical sorption. Thermodynamic parameters of the process showed that the adsorption process was spontaneous and endothermic. Structural changes of raw and acid-treated samples were characterized by FTIR, XRD and BET analyses, and then their performances for zinc removal were compared. The results showed that acid activation of bentonite reduced the maximum elimination of zinc ions by approximately 50–60 %. In this study, Artificial Neural Networks (ANN) were tested to observe the effect of different parameters on the adsorption of zinc from aqueous media with bentonite. It was observed that the number of neurons in the hidden layer and the selected functions were effective in the excellent performance of ANN. The tested networks were exhibited superior fitting in predicting the adsorption process at different numbers of neurons.

CRediT authorship contribution statement

Ezel Uraz: Validation, Methodology, Investigation, Formal analysis, Writing – original draft. **Tugba Hayri-Senel:** Writing – original draft, Validation, Methodology, Investigation, Formal analysis. **Nalan Erdol-Aydin:** Resources, Investigation, Writing – review & editing. **Gulhayat Nasun-Saygili:** Writing – review & editing, Supervision, Resources, Methodology.

Data statement

Data will be made available on request.

Declaration of competing interest

The authors declare that they have no known competing financial interests or personal relationships that could have appeared to influence the work reported in this paper.

Acknowledgements

This study was supported by Istanbul Technical University Scientific Research Projects Unit (Grant: FHD-2024-45977).

References

[1] S. Hussain, S. Malik, M.J. Masud Cheema, M.U. Ashraf, M.S. Waqas, M.M. Iqbal, S. Ali, L. Anjum, M. Aslam, H. Afzal, An overview on emerging water scarcity challange in pakistan, its consumption, causes, impacts and remedial measures, big data, Water Resources Engineering (BDWRE) 1 (2020) 22–31, https://doi.org/10.26480/bdwre.01.2020.22.31.
[2] A. Abdul Sattar, Preparation of novel hybrid (almond shell and pleurotus sajor caju) biosorbent for the removal of heavy metals (nickel and lead) from wastewater, Water Conservation & Management 5 (2020) 1–7, https://doi.org/10.26480/wcm.01.2021.01.07.
[3] S. Sudhakar, N. Moondra, R.A. Christian, A comparative study on treatment of CETP wastewater using SBR and SBR-IFAS process, Water Conservation & Management 6 (2022) 51–54.
[4] Ş. Şehnaz, E. Şener, A. Davraz, S. Varol, Hydrogeological and hydrochemical investigation in the burdur saline lake basin, southwest Turkey, Geochemistry 80 (2020) 125592, https://doi.org/10.1016/j.chemer.2019.125592.
[5] K. Tohdee, L. Kaewsichan, Asadullah, Enhancement of adsorption efficiency of heavy metal Cu(II) and Zn(II) onto cationic surfactant modified bentonite, J. Environ. Chem. Eng. 6 (2018) 2821–2828, https://doi.org/10.1016/j.jece.2018.04.030.
[6] Y. Xue, Y. Ma, G. Long, H. He, Z. Li, Z. Yan, B. Zhu, Evaluation of water quality pollution and analysis of vertical distribution characteristics of typical Rivers in the Pearl River Delta, South China, J. Sea Res. 193 (2023).
[7] J.U.K. Oubagaranadin, Z.V.P. Murthy, V.P. Mallapur, Removal of Cu(II) and Zn(II) from industrial wastewater by acid-activated montmorillonite-illite type of clay, Compt. Rendus Chem. 13 (2010) 1359–1363, https://doi.org/10.1016/j.crci.2010.05.024.
[8] A. Daraei, Treatment of textile waste water with organoclay, Iran J, Chemical Engineering 32 (2013) 67–70.
[9] S. Zhu, Y. Zhang, L. Xin, K. Htet Oo, M. Zheng, S. Ma, J. Guo, Y. Chen, Near-complete recycling of real mix electroplating sludge as valuable metals via Fe/Cr co-crystallization and stepwise extraction route, J Environ Manage 358 (2024) 120821, https://doi.org/10.1016/j.jenvman.2024.120821.
[10] Y. Shen, P. Sun, L. Ye, D. Xu, Progress of anaerobic membrane bioreactor in municipal wastewater treatment, Sci. Adv. Mater. 15 (2023) 1277–1298, https://doi.org/10.1166/sam.2023.4531.
[11] G. Bouazza, S. Souabi, A. Madinzi, E.H. Chatri, Optimization of the color corresponding to the different absorbencies of tannery wastewater by response surface designs, Water Conservation & Management 6 (2022) 99–106.
[12] X.P.N. Nguyen, D.T. Nguyen, V.V. Pham, V.D. Bui, Evaluation of the synergistic effect in wastewater treatment from ships by the advanced combination system, Water Conservation & Management 5 (2021) 60–65, https://doi.org/10.26480/wcm.01.2021.60.65.
[13] K.D. Abdulwahid, Phytoremediation of cadmium pollutants in wastewater by using ceratophyllum demersum L. As an aquatic macrophytes, Water Conservation & Management 7 (2023) 83–88, https://doi.org/10.26480/wcm.02.2023.83.88.
[14] R. Prasad, K.D. Yadav, Use of response surface methodology and artificial neural network approach for methylene blue removal by adsorption onto water hyacinth, Water Conservation and Management 4 (2020) 83–89, https://doi.org/10.26480/wcm.02.2020.83.89.
[15] A. Alemu, B. Lemma, N. Gabbiye, M.T. Alula, M.T. Desta, Removal of chromium (VI) from aqueous solution using vesicular basalt: a potential low-cost wastewater treatment system, Heliyon (2018) e00682.
[16] T.A. Bullo, Y.M. Bayisa, Optimizing the removal efficiency of chromium from tanning plant effluent by adsorption method with activated carbon chat stems (catha edulis) using response surface methodology, Water Conservation & Management 6 (2022) 15–21, https://doi.org/10.26480/wcm.01.2022.15.21.
[17] A. Salem, M. Saghapour, Effect of activation factors on adsorption of methylene blue by modified bentonite, Progress in Color Colorants Coating 6 (2013) 97–108.
[18] R. Francisco, D. Valenzuela, Studies on the acid activation of Brazilian smectitic clays, Quim. Nova 24 (2001) 345–353.
[19] M. Kashani, A. Youzbashi, Z. Amiri Rigi, Effect of acid activation on structural and bleaching properties of a bentonite, Iranian Journal of Materials Science&Engineering 8 (2011) 50–56.
[20] A. Mellah, S. Chegrouche, The removal of zinc from aqueous solutions by natural bentonite, Water Res. 31 (1997) 621–629, https://doi.org/10.1016/S0043-1354(96)00294-1.

[21] E. Álvarez-Ayuso, A. García-Sánchez, Removal of heavy metals from waste waters by natural and Na-exchanged bentonites, Clays Clay Miner 51 (2003) 475–480, https://doi.org/10.1346/CCMN.2003.0510501.

[22] S. Lin, Heavy metal removal from water by sorption using surfactant-modified montmorillonite, J. Hazard Mater. 92 (2002) 315–326, https://doi.org/10.1016/S0304-3894(02)00026-2.

[23] B. Bayat, Comparative study of adsorption properties of Turkish fly ashes, J. Hazard Mater. 95 (2002) 251–273, https://doi.org/10.1016/S0304-3894(02)00140-1.

[24] K.G. Bhattacharyya, S. Sen Gupta, Adsorption of a few heavy metals on natural and modified kaolinite and montmorillonite: a review, Adv. Colloid Interface Sci. 140 (2008) 114–131, https://doi.org/10.1016/j.cis.2007.12.008.

[25] T.K. Sen, D. Gomez, Adsorption of zinc (Zn2+) from aqueous solution on natural bentonite, Desalination 267 (2011) 286–294, https://doi.org/10.1016/j.desal.2010.09.041.

[26] A. Debnath, K. Deb, N.S. Das, K.K. Chattopadhyay, B. Saha, Simple chemical route synthesis of Fe $_2$ O $_3$ nanoparticles and its application for adsorptive removal of Congo red from aqueous media: artificial neural network modeling, J Dispers Sci Technol 37 (2016) 775–785, https://doi.org/10.1080/01932691.2015.1062772.

[27] R. Alrowais, M.M. Abdel daiem, B.M. Nasef, N. Said, Activated carbon fabricated from biomass for adsorption/bio-adsorption of 2,4-D and MCPA: kinetics, isotherms, and artificial neural network modeling, Sustainability 16 (2023) 299, https://doi.org/10.3390/su16010299.

[28] I. Dahlan, E.E.M. Azhar, S.R. Hassan, H.A. Aziz, Y.-T. Hung, Statistical modeling and optimization of process parameters for 2,4-dichlorophenoxyacetic acid removal by using AC/PDMAEMA hydrogel adsorbent: comparison of different RSM designs and ANN training methods, Water (Basel) 14 (2022) 3061, https://doi.org/10.3390/w14193061.

[29] S. Malamis, E. Katsou, A review on zinc and nickel adsorption on natural and modified zeolite, bentonite and vermiculite: examination of process parameters, kinetics and isotherms, J. Hazard Mater. 252–253 (2013) 428–461, https://doi.org/10.1016/j.jhazmat.2013.03.024.

[30] S. Pandey, A comprehensive review on recent developments in bentonite-based materials used as adsorbents for wastewater treatment, J. Mol. Liq. 241 (2017) 1091–1113, https://doi.org/10.1016/j.molliq.2017.06.115.

[31] H. Liu, T. Fu, M.T. Sarwar, H. Yang, Recent progress in radionuclides adsorption by bentonite-based materials as ideal adsorbents and buffer/backfill materials, Appl. Clay Sci. 232 (2023) 106796, https://doi.org/10.1016/j.clay.2022.106796.

[32] E.Y. Choi, R. Graham, J. Stangoulis, Semi-quantitative analysis for selecting Fe- and Zn-dense genotypes of staple food crops, J. Food Compos. Anal. 20 (2007) 496–505, https://doi.org/10.1016/j.jfca.2007.01.004.

[33] A. Kocyła, A. Pomorski, A. Krężel, Molar absorption coefficients and stability constants of Zincon metal complexes for determination of metal ions and bioinorganic applications, J. Inorg. Biochem. 176 (2017) 53–65, https://doi.org/10.1016/j.jinorgbio.2017.08.006.

[34] H. He, W. Zhang, S. Ye, S. Li, Z. Nie, Y. Zhang, M. Xiong, W.-T. Chen, G. Hu, Magnetical multi-walled carbon nanotubes with Lewis acid-base imprinted sites for efficient Ni(II) recovery with high selectivity, Surface. Interfac. 48 (2024) 104383, https://doi.org/10.1016/j.surfin.2024.104383.

[35] W.K. Mekhamer, Stability changes of Saudi bentonite suspension due to mechanical grinding, J. Saudi Chem. Soc. 15 (2011) 361–366, https://doi.org/10.1016/j.jscs.2011.03.014.

[36] A. Kaya, A.H. Oren, Adsorption of zinc from aqueous solutions to bentonite, J. Hazard Mater. 125 (2005) 183–189, https://doi.org/10.1016/j.jhazmat.2005.05.027.

[37] L.A.S.J. Carvalho, R.A. Konzen, A.C.M. Cunha, P.R. Batista, F.J. Bassetti, L.A. Coral, Efficiency of activated carbons and natural bentonite to remove direct orange 39 from water, J. Environ. Chem. Eng. 7 (2019) 103496, https://doi.org/10.1016/j.jece.2019.103496.

[38] F.W. Mahatmanti, J. Jumaeri, E. Kusumastuti, The adsorption behavior of individual Cu(II), Zn(II), and Cd(II) ions over a CuO-modified ceramic membrane synthesized from fly ash, J. King Saud Univ. Sci. 35 (2023) 102866, https://doi.org/10.1016/j.jksus.2023.102866.

[39] K. Bellir, M.B. Lehocine, A.-H. Meniai, Zinc removal from aqueous solutions by adsorption onto bentonite, Desalination Water Treat. 51 (2013) 5035–5048, https://doi.org/10.1080/19443994.2013.808786.

[40] A.H. Alabi, V.A. Adekunle, A.A. Azeez, B.W. Akinwale, C.A. Olanrewaju, P.O. Oladoye, K.S. Obayomi, Sequestration of divalent heavy metal ions from aqueous environment by adsorption using biomass-bentonite composites as potential adsorbent: equilibrium and kinetic studies, Nano-Structures & Nano-Objects 38 (2024) 101183, https://doi.org/10.1016/j.nanoso.2024.101183.

[41] M.E. Küçük, I. Makarava, T. Kinnarinen, A. Häkkinen, Simultaneous adsorption of Cu(II), Zn(II), Cd(II) and Pb(II) from synthetic wastewater using NaP and LTA zeolites prepared from biomass fly ash, Heliyon 9 (2023) e20253, https://doi.org/10.1016/j.heliyon.2023.e20253.

[42] D. Abdissa, K. Beyecha, Sugarcane bagasse adsorptıon evaluatıon and applıcatıon on bod and cod removal from textıle wastewater treatment, Water Conservatıon & Management 5 (2020) 30–34, https://doi.org/10.26480/wcm.01.2021.30.34.

[43] H. Noyan, M. Onal, Y. Sarıkaya, The effect of sulphuric acid activation on the crystallinity, surface area, porosity, surface acidity, and bleaching power of a bentonite, Food Chem. 105 (2007) 156–163, https://doi.org/10.1016/j.foodchem.2007.03.060.

[44] A. Oren, A. Kaya, Factors affecting adsorption characteristics of Zn2+ on two natural zeolites, J. Hazard Mater. 131 (2006) 59–65, https://doi.org/10.1016/j.jhazmat.2005.09.027.

[45] S. Veli, B. Alyüz, Adsorption of copper and zinc from aqueous solutions by using natural clay, J. Hazard Mater. 149 (2007) 226–233, https://doi.org/10.1016/j.jhazmat.2007.04.109.

[46] H. Zhang, Z. Tong, T. Wei, Y. Tang, Removal characteristics of Zn(II) from aqueous solution by alkaline Ca-bentonite, Desalination 276 (2011) 103–108, https://doi.org/10.1016/j.desal.2011.03.026.

[47] N.G. Turan, S. Elevli, B. Mesci, Adsorption of copper and zinc ions on illite: determination of the optimal conditions by the statistical design of experiments, Appl. Clay Sci. 52 (2011) 392–399, https://doi.org/10.1016/j.clay.2011.04.010.

[48] M. Fu, X. Tuo, X. Yan, D. Li, H. Zhu, S. Gao, X. Han, J. Zhou, D. Mou, J. Xiu, Adsorption performance and mechanism of pectin modified with β-cyclodextrin for Zn2+ and Cu2+, Int. J. Biol. Macromol. 274 (2024) 133563 https://doi.org/10.1016/j.ijbiomac.2024.133563.

[49] X. Sun, B. Peng, Y. Ji, J. Chen, D. Li, Chitosan(chitin)/cellulose composite biosorbents prepared using ionic liquid for heavy metal ions adsorption, AIChE J. 55 (2009) 2062–2069, https://doi.org/10.1002/aic.11797.

[50] W. Pranata Putra, A. Kamari, S. Najiah Mohd Yusoff, C. Fauziah Ishak, A. Mohamed, N. Hashim, I. Md Isa, Biosorption of Cu(II), Pb(II) and Zn(II) ions from aqueous solutions using selected waste materials: adsorption and characterisation studies, J. Encapsulation Adsorpt. Sci. 4 (2014) 25–35, https://doi.org/10.4236/jeas.2014.41004.

[51] Ş. Kubilay, R. Gürkan, A. Savran, T. Şahan, Removal of Cu(II), Zn(II) and Co(II) ions from aqueous solutions by adsorption onto natural bentonite, Adsorption 13 (2007) 41–51, https://doi.org/10.1007/s10450-007-9003-y.

[52] P. Wijeyawardana, N. Nanayakkara, D. Law, C. Gunasekara, A. Karunarathna, B.K. Pramanik, Evaluating the performance of cement-modified biochar adsorbent for Cu, Pb and Zn removal from urban stormwater, Process Saf. Environ. Protect. 186 (2024) 1419–1431, https://doi.org/10.1016/j.psep.2024.04.126.

[53] M. Zhao, Y. Dai, M. Zhang, C. Feng, B. Qin, W. Zhang, N. Zhao, Y. Li, Z. Ni, Z. Xu, D.C.W. Tsang, R. Qiu, Mechanisms of Pb and/or Zn adsorption by different biochars: biochar characteristics, stability, and binding energies, Sci. Total Environ. 717 (2020) 136894, https://doi.org/10.1016/j.scitotenv.2020.136894.

[54] S. Biswas, T.K. Sen, A.M. Yeneneh, B.C. Meikap, Synthesis and characterization of a novel Ca-alginate-biochar composite as efficient zinc (Zn $^{2+}$) adsorbent: thermodynamics, process design, mass transfer and isotherm modeling, Sep Sci Technol 54 (2019) 1106–1124, https://doi.org/10.1080/01496395.2018.1527353.

[55] R. Shahrokhi-Shahraki, C. Benally, M.G. El-Din, J. Park, High efficiency removal of heavy metals using tire-derived activated carbon vs commercial activated carbon: insights into the adsorption mechanisms, Chemosphere 264 (2021) 128455, https://doi.org/10.1016/j.chemosphere.2020.128455.

[56] S. Satouh, S. Bousba, N. Bougdah, C.E. Bounoukta, S. Halladja, N. Messikh, A Ziziphus jujuba waste-derived biochar as a low-cost adsorbent for the removal of Indigo carmine dye from aqueous solution, Desalination Water Treat. 289 (2023) 258–270, https://doi.org/10.5004/dwt.2023.29445.

[57] A.S. Saadi, S. Bousba, A. Riah, M. Belghit, B. Belkhalfa, H. Barour, Efficient synthesis of magnetic activated carbon from oak pericarp for enhanced dye adsorption: a one-step approach, Desalination Water Treat. 319 (2024) 100420, https://doi.org/10.1016/j.dwt.2024.100420.

[58] Y.S. Chang, P.I. Au, N.M. Mubarak, M. Khalid, P. Jagadish, R. Walvekar, E.C. Abdullah, Adsorption of Cu(II) and Ni(II) ions from wastewater onto bentonite and bentonite/GO composite, Environ. Sci. Pollut. Control Ser. 27 (2020) 33270–33296, https://doi.org/10.1007/s11356-020-09423-7.
[59] L. Zhirong, Md Azhar Uddin, S. Zhanxue, FT-IR and XRD analysis of natural Na-bentonite and Cu(II)-loaded Na-bentonite, Spectrochim. Acta Mol. Biomol. Spectrosc. 79 (2011) 1013–1016, https://doi.org/10.1016/j.saa.2011.04.013.
[60] K. Atkovska, B. Bliznakovska, G. Ruseska, S. Bogoevski, B. Boskovski, A. Grozdanov, Adsorptıon of Fe(Iı) And Zn(Iı) Ions from Landfill Leachate by natural bentonıte, Journal of Chemical Technology & Metallurgy 51 (2016) 215–222.
[61] E.G. Pradas, M.V. Sánchez, F.C. Cruz, M.S. Viciana, M.F. Pérez, Adsorption of cadmium and zinc from aqueous solution on natural and activated bentonite, Journal of Chemical Technology & Biotechnology 59 (1994) 289–295, https://doi.org/10.1002/jctb.280590312.
[62] S.T. Akar, Y. Yetimoglu, T. Gedikbey, Removal of chromium (VI) ions from aqueous solutions by using Turkish montmorillonite clay: effect of activation and modification, Desalination 244 (2009) 97–108, https://doi.org/10.1016/j.desal.2008.04.040.
[63] E. Heraldy, W.W. Lestari, D. Permatasari, D.D. Arimurti, Biosorbent from tomato waste and apple juice residue for lead removal, J. Environ. Chem. Eng. 6 (2018) 1201–1208, https://doi.org/10.1016/j.jece.2017.12.026.
[64] Y.-S. Ho, A.E. Ofomaja, Biosorption thermodynamics of cadmium on coconut copra meal as biosorbent, Biochem. Eng. J. 30 (2006) 117–123, https://doi.org/10.1016/j.bej.2006.02.012.
[65] N. Febriana, S.O. Lesmana, F.E. Soetaredjo, J. Sunarso, S. Ismadji, Neem leaf utilization for copper ions removal from aqueous solution, J. Taiwan Inst. Chem. Eng. 41 (2010) 111–114, https://doi.org/10.1016/j.jtice.2009.04.003.
[66] A. Bhatnagar, E. Kumar, A.K. Minocha, B.-H. Jeon, H. Song, Y.-C. Seo, Removal of anionic dyes from water using *Citrus limonum* (lemon) peel: equilibrium studies and kinetic modeling, Sep Sci Technol 44 (2009) 316–334, https://doi.org/10.1080/01496390802437461.
[67] T.A. Khan, M. Nazir, I. Ali, A. Kumar, Removal of Chromium(VI) from aqueous solution using guar gum–nano zinc oxide biocomposite adsorbent, Arab. J. Chem. 10 (2017) S2388–S2398, https://doi.org/10.1016/j.arabjc.2013.08.019.
[68] V. Gopal, P. Elango, Kinetic and thermodynamic investigations of adsorption of fluoride onto activated vera carbon, J. Indian Chem. Soc. 84 (2007) 1114–1118.
[69] T.S. Silva, M. de Freitas Souza, T. Maria da Silva Teófilo, M. Silva dos Santos, M.A. Formiga Porto, C.M. Martins Souza, J. Barbosa dos Santos, D.V. Silva, Use of neural networks to estimate the sorption and desorption coefficients of herbicides: a case study of diuron, hexazinone, and sulfometuron-methyl in Brazil, Chemosphere 236 (2019) 124333, https://doi.org/10.1016/j.chemosphere.2019.07.064.
[70] S. H, R. Bhat M, R. Selvaraj, Removal of an agricultural herbicide (2,4-Dichlorophenoxyacetic acid) using magnetic nanocomposite: a combined experimental and modeling studies, Environ. Res. 238 (2023) 117124, https://doi.org/10.1016/j.envres.2023.117124.
[71] N. Messikh, S. Bousba, N. Bougdah, The use of a multilayer perceptron (MLP) for modelling the phenol removal by emulsion liquid membrane, J. Environ. Chem. Eng. 5 (2017) 3483–3489, https://doi.org/10.1016/j.jece.2017.06.053.
[72] N. Bougdah, S. Bousba, Y. Belhocine, N. Messikh, Application of multilayer perceptron network and random forest models for modelling the adsorption of chlorobenzene on a modified bentonite by intercalation with hexadecyltrimethyl ammonium (HDTMA), React. Kinet. Mech. Catal. 135 (2022) 247–270, https://doi.org/10.1007/s11144-021-02121-6.